

# Thunderstorm-Generated Solitary Waves: A Wind Shear Hazard

R. J. Doviak\*

*National Oceanic and Atmospheric Administration, Norman, Oklahoma  
and*

D. R. Christief

*Australian National University, Canberra, Australia*

Observations of a boundary-layer solitary wave sensed with the National Severe Storms Laboratory's Doppler weather radar and a 444-m-tall instrumented tower suggest that solitary and other nonlinear waves are a source of significant wind shear hazard to safe flight and thus should be studied both experimentally and theoretically. Wave transport of the horizontal momentum of the vertically sheared ambient air contributed much to the observed wind perturbations and horizontal wind shear. Observations are compared with, and shown to agree fairly closely with, the waveform predicted by steady state, weakly nonlinear, internal wave theory.

## Introduction

THE introduction of new observational devices (e.g., Doppler radar,<sup>1</sup> airborne Doppler lidar<sup>2</sup>) and improvements in conventional techniques (e.g., meteorological instruments on tall towers<sup>3</sup>) are leading to new insights and an understanding of a variety of thunderstorm phenomena that are hazardous to safe flight. Thunderstorm outflows are particularly dangerous to jet aircraft because of their high wing loading, and because of the delay in thrust of the engines after power is applied.<sup>4</sup>

Research at the National Center for Atmospheric Research and the University of Chicago has made the aviation community aware of wind shear hazards accompanying damaging downdrafts, recently called downbursts or, if of small diameter (i.e., 0.4–4 km; 1300–13,000 ft), microbursts.<sup>5,6</sup> However, these are not the only weather phenomena that can contain wind shear dangerous to an aircraft on its ascent from or descent into air terminals. Tornadoes and/or their larger diameter parent circulations, called mesocyclones, have caused crashes. On October 6, 1981, a Fokker F-28 commercial aircraft was observed exiting a thunderstorm cloud base at the location of a tornado that apparently sheared a wing from its fuselage.

Gust fronts, usually associated with the leading edge of thunderstorm-generated density currents, have been identified for a long time as a region of low altitude wind shear dangerous to safe flight.<sup>7</sup> It has also been known for many years that thunderstorm downdrafts, the source of these ground-level currents, harbor winds that are dangerous to aircraft. The principal hazard of the microburst, however, is not necessarily confined to the direct effects of the downdraft. As Lee et al.<sup>8</sup> pointed out, the aircraft is passing beneath a downdraft "experiences first a strong headwind, then roughly no horizontal wind at all as it enters the downflow area, and finally experiences a strong tailwind. These wind shifts from headwind to

tailwind, with a vector difference of 40 m/s or more in 4 km in the horizontal, may be more dangerous than the well-organized gust front."

Much of the earlier research on wind shear focused attention on the gust front of the density current. However, it is now known that gust fronts and associated thin lines of reflectivity are observed at the leading edge of bores<sup>9</sup> and solitary waves<sup>10</sup> as well as density currents. The Federal Aviation Administration has deployed a network of anemometers (i.e., the Low Level Wind Shear Alert System, LLWAS) to detect these traveling gusts and to estimate their horizontal shear.<sup>11</sup> In its simplest form, a density current is a shallow layer of laminar flow having a leading edge that moves at a velocity dependent upon the depth of the current as well as the difference in density (or temperature) of the ambient fluid and that within the current.<sup>12</sup> If this description applied to atmospheric density currents, the wind shear hazards would be minimal because aircraft would experience only a net increase in headwind. However, currents are not necessarily laminar and they often have at their leading edge a mass of recirculating air (called a density or gravity current head) that is somewhat deeper than the current behind it; this propagating horizontal rotor with its pattern of increasing and decreasing head or tail wind is the primary source of hazardous wind shear. Wind gusts generated by these rotors can have their vorticity (shear) magnified as it is being stretched by the radially diverging outflow.<sup>13</sup> Evidence suggests that this zone of shear could be more dangerous to safe flight than the wind change encountered across the microburst itself.

One of the earliest accidents that has been attributed to changes in head wind is that reported in 1958 by Stewart, who described a "microburst-type" wind shear event (Fig. 1) that downed a BOAC Argonaut on its takeoff from the Kano Airport in Nigeria in June 1956.<sup>14</sup> The investigating board concluded that, "The accident was the result of the loss of height and airspeed caused by the aircraft encountering, at approximately 250 ft after take-off, an unpredictable thunderstorm cell that gave rise to a sudden reversal of wing direction, heavy rain, and possible downdraft condition."

Hazardous low-altitude shear has been associated with mountain lee waves, sea breezes, cold frontal passages, and more recently, with large-amplitude gravity (or buoyancy) wave disturbances.<sup>15</sup> Gossard observed gravity waves that had wind speed changes as much as 20 m/s (40 knots) in a distance of 5 km (3 mi).<sup>16</sup>

Received Dec. 14, 1987; presented as Paper 88-0695 at the AIAA 26th Aerospace Sciences Meeting, Reno, NV, Jan. 11-14, 1988; revision received Aug. 23, 1988. This paper is declared a work of the U.S. Government and is not subject to copyright protection in the United States.

\*Senior Scientist, Environmental Research Laboratories, National Severe Storms Laboratory.

†Research School of Earth Science, Institute of Advanced Studies.

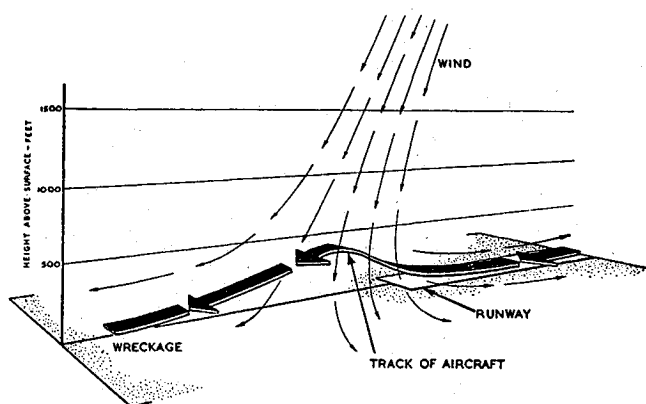


Fig. 1 Unusual conditions that led to the Kano accident in 1956.

In this paper, we focus our attention on gravity waves that have large amplitude yet short width (wavelength) and, consequently, strong shear, but that are exceptionally stable and can travel hundreds of kilometers from the source with relatively little attenuation of the possibly hazardous shear. These gravity waves, known as solitary waves,<sup>17</sup> have recently been identified as a significant source of low-altitude shear.<sup>18-20</sup>

The ease with which solitary waves can be generated in fluids in the laboratory suggests that large-amplitude nonlinear waves might be a commonly occurring feature in the lowest part of the troposphere whenever suitable boundary-layer conditions exist and sources are active.<sup>21</sup> The first definitive observations of short wavelength atmospheric solitary waves in the planetary boundary layer were made in 1976 at the Australian National University's Warramunga Infrasonic Array near Tennant Creek in Northern Australia. The origin of many of these waves can be attributed to the interaction of a deeply penetrating Gulf of Carpentaria sea breeze front with an intense nocturnal inversion.

Solitary waves are most commonly observed with amplitudes of 300–1000 m (900–3000 ft) and effective horizontal lengths of 0.5–7 km (0.3–5 mi). They usually propagate with speeds between 6 and 16 m/s (12 and 32 knots) but, on occasion, they have been observed to propagate with speeds exceeding 30 m/s (60 knots). Atmospheric solitary waves propagate along horizontal waveguides formed by the strong temperature inversion of stably stratified layers. Solitary waves can grow in amplitude as their width decreases, thereby increasing shear, and their speed exceeds the speed of long-wavelength weak disturbances by an amount proportional to wave amplitude.<sup>22</sup> Thus, solitary waves have supercritical speeds. Wind shear in large-amplitude solitary waves is enhanced by the presence of recirculating flow within the wave that leads to wave-induced horizontal winds near the surface that exceed the speed of the wave.

Long-wavelength disturbances of very small amplitude experience little dispersion and accompanying change in shape, resulting in long lifetimes. Short-wavelength disturbances of small amplitude, on the other hand, experience significant dispersion and thereby disintegrate quickly. However, short wavelength disturbances of large amplitude can evolve into waves of permanent form under the influence of amplitude dispersion. In other words, the tendency of a large-amplitude disturbance to steepen and break because of nonlinearity is offset by normal frequency dispersion, which tends to smooth the disturbance. Solitary waves are therefore unusually stable large-amplitude disturbances that can carry intense shear long distances.

We show results of observations suggesting that shear generated by solitary waves can have a significant effect on aircraft performance. Solitary waves that produce low-altitude wind shear require strong stability of the atmosphere close to the Earth's surface and near-neutral stability above.<sup>23</sup> Thus, it is

likely that many significant events may pass unobserved because such stable conditions usually occur in the late night or early morning hours when observations are sparse. On the other hand, thunderstorm outflows can form stable layers at any time and subsequent thunderstorm downdrafts, impinging onto this layer, can initiate large-amplitude gravity waves, as observed by Doviak and Ge.<sup>10</sup> It must be expected therefore that solitary wave wind shear may be encountered at any time over the airport region when widespread thunderstorm conditions prevail. In this context, it is worth noting that some pilots and other members of the aviation community have long recognized that new, and seemingly benign, cell formations are often more violent than the present storm.<sup>24</sup> A good example where conditions of this type have led to tragedy is the Dallas-Fort Worth storm that caused the crash of Delta 191 in 1985 (e.g., see Fig. 1.20 of Fujita<sup>25</sup>). It has been recommended in the Safety Digest of the 1960 issue of *Skyways* that "if it begins to rain in the direct take-off flight path, close to but separated from the main storm, it is prudent to remain on the ground until it has passed away."<sup>24</sup>

Solitary waves might be one of the most insidious forms of wind shear because they usually occur, without warning, as unexpected clear-air disturbances, invisible to the naked eye and far from any storms. Yet they can harbor shears that might be destructive to aircraft and crew. Although there is no documentation with conclusive evidence linking solitary waves to crashes, there are accidents in which solitary waves cannot be dismissed as the cause. For example, a study by Anderson and Clark shows that, of 43 meteorologically related wind shear incidents in Australia, only 16% could be attributed with any certainty to frontal and thunderstorm activity.<sup>26,27</sup> Thus, considering the insidious nature of solitary waves and their frequency of occurrence, Christie and Muirhead<sup>18</sup> inferred that it is reasonable to assume that many of the remaining incidents, and quite possibly some of the former, can be attributed to solitary wave activity in the first few hundred meters of the atmospheric boundary layer. It is to be emphasized that the horizontal wind shear associated with the wave is strongest near the ground where aircraft are most vulnerable.

The effect of a solitary wave on aircraft performance is complicated because it depends on the pilot's response to physical stimuli. Furthermore, the response depends on the direction of approach into the wave. For example, Fig. 2 reproduces the streamlines of a numerically modeled and an observed solitary wave on which is superimposed a 3 deg glide path for an aircraft approaching the wave propagating toward it. The streamlines are drawn for the wind relative to a coordinate frame that moves with the wave. For this case, it can be deduced that the aircraft would first experience an increase in head wind and updraft followed by a decrease in head wind and downdraft. The short-dashed line suggests the flight path that could result as a consequence of aircraft response to the effects of shear. For aircraft approaching from the opposite direction, the flight path would initially be below the glide

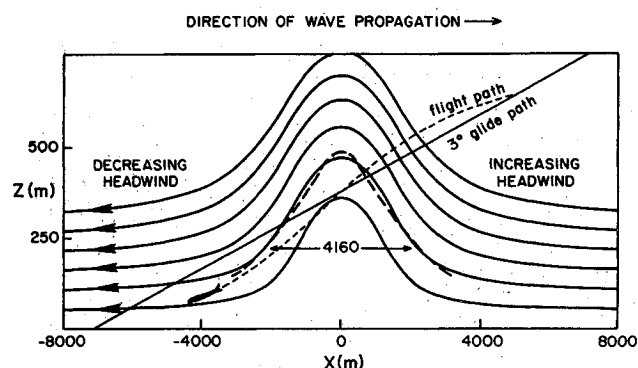


Fig. 2 Hypothetical aircraft encounter with a solitary wave (solid streamlines are from numerical model, dashed streamline is from observation<sup>10,15</sup>).

path and then (if the aircraft is still airborne) above, with the possibility that the aircraft would overshoot the runway.

The wind profile along a glide slope through a solitary wave in a shearless environment differs from that encountered in a microburst because a single-crested solitary wave produces only an increase in head wind (or tail wind) and then decreases to the initial wind state, whereas the microburst generates both head and tail wind components. That is, the horizontal wind shift is unimodal in a solitary wave, whereas it is bimodal in a microburst. However, a sequence of two or more solitary waves can evolve from an undular bore (to be shown later in Fig. 10) and this can give the pilot the appearance of alternating head and tail wind components, thus making control of the aircraft more difficult. On the other hand, wind shear effects along glide slopes can resemble those associated with a microburst, if flights are made through a solitary wave in a vertically sheared environmental wind.

### Observations

Doviak and Ge<sup>10</sup> presented evidence that a thin line of reflectivity commonly associated with gust fronts was in fact a solitary wave generated by the interaction of thunderstorm outflows. However, they did not make quantitative comparisons of data with theory. In the following sections, we examine in greater detail data from a tall (444 m) television (KTVY) tower, instrumented by the National Severe Storms Laboratory, to determine the waveform to be compared with that deduced from two-dimensional weakly nonlinear theory of solitary waves.

### The Ambient Environment

It can be shown that it is the virtual potential temperature  $\theta_{v0}$  of the unsaturated ambient atmosphere that determines its stability and hence its period of a buoyancy oscillation. A strongly stable layer embedded in an atmosphere having a

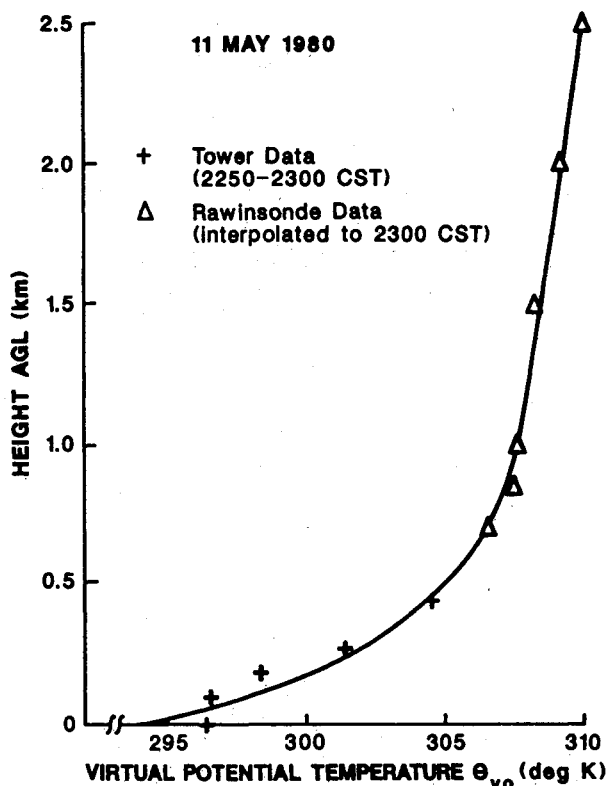


Fig. 3 Virtual potential temperature vs height above ground level (AGL) circa 22:55 CST on May 11, 1980.

much longer period of buoyancy oscillation conducts large-amplitude gravity wave disturbances long distances from their source. The  $\theta_{v0}$  is related to the sensible temperature  $T$  (i.e., the dry bulb temperature in K) and the ratio  $w$  of water vapor to dry air density (i.e., the mixing ratio in grams per gram) by the equation

$$\theta_{v0} = \left( \frac{1 + 1.61w}{1 + w} \right) T \left( \frac{1000}{p} \right)^{0.286(1 - 0.23w)}$$

where  $p$  is pressure in millibar units. To compute the vertical profile of  $\theta_{v0}$  (Fig. 3), the measured  $T$  and pressure were used to relate the pressure heights of the rawinsondes to real heights in meters above the ground. It was noted that if a standard atmosphere was used to obtain this relation, height errors larger than 100 m above 2 km and thus temperature errors of about 1 K or more would have occurred.

The profile (Fig. 3) in advance of the wave is calculated from data obtained with tall tower instruments up to 444 m and from rawinsondes for higher altitudes by interpolating data at the 18:00 CST (Central Standard Time) 5/11/80 and 06:00 CST 5/12/80 sounding times to the 23:00 CST time of wave passage at the tower. The  $\theta_{v0}$  computed from tower data show the presence of an intensely stable surface-based layer having a thickness of at least several hundred meters topped by a weakly stratified region.

Figure 4 shows the vertical profiles of the ambient wind components normal to ( $u_a$ ) and parallel to ( $v_a$ ) the wave front before the time (23:05-23:15) the wave passes the tower. The estimates from anemometers ( $\Delta$ ) on the tower (36 km from the radar at azimuth 356 deg) are 10 min averages of the data spaced 10 s apart about 22:45, the time Doppler radar data were also used to compute  $u$  and  $v_a$ .

The ambient winds measured with radar ( $\circ$  in Fig. 4) are obtained from estimated Doppler velocities for an assumed horizontally uniform wind model, least-squares fitted to the Doppler velocities measured over an azimuthal sector from 330 to 30 deg at ranges near 30 to 40 km where data were free from ground clutter and range-aliased overlying echoes. The horizontal bars indicate the 95% confidence limits, assuming errors are Gaussian distributed and using the computed rms values of the data about the model velocity. The vertical bars denote the uncertainty in beam height for a 0.1 deg uncertainty in elevation angle and also the variation in beam height because radar data from a 4 km range interval were used in the fitting. The solid lines in Fig. 4 are the inferred profiles of the ambient wind,  $u_a$  and  $v_a$ .

The winds measured by rawinsonde (+ in Fig. 4) are values interpolated from sounding data at 18:00 on May 11 and 06:00 on May 12. Although the interpolated temperature profile appears to reasonably estimate the ambient temperature above the stable layer because there is less than a 2°C change over the 12 h interval between soundings, the wind field changes considerably during this interval and the interpolated wind differs significantly from the radar-derived wind. Nevertheless, there is good agreement between tower- and radar-measured winds that are from data close to the same time.

The difference in wind measured by the radar and tower at the common height of 400 m is most likely due to the combined effects of reflectivity gradients, beamwidth, beam blockage, and nonuniformity of the wind that was assumed in the model used to fit the Doppler data. For example, Fig. 4 shows the ambient wind profile  $v_0$  averaged for the 2 min period just preceding the solitary wave at the tower. We assume that this  $v_0$  profile represents the values that the ambient wind would have if the wave were not present.

### Equivalent Potential Temperature

The equivalent potential temperature  $\theta_e$  is the final temperature of an air parcel after it is lifted dry adiabatically to its lifting condensation level, then pseudowet adiabatically to a

great height to condense water as it is formed, and finally brought down dry adiabatically to a reference pressure of 1000 mbar.<sup>28</sup> The  $\theta_e$  is a conserved property of the air parcel even with the change of moisture phase as would occur if a cloud is formed when nearly saturated air is lifted by the wave.

The  $\theta_e$  is not so easy to compute. An approximate formula<sup>29</sup> is

$$\theta_e \approx \theta e^{L(T_s)w_s/c_p T_s}$$

where  $\theta$  is the potential temperature that a parcel of unsaturated air would have if brought adiabatically to a reference pressure of 1000 mbar,  $L$  the latent heat of condensation at  $T_s$ ,

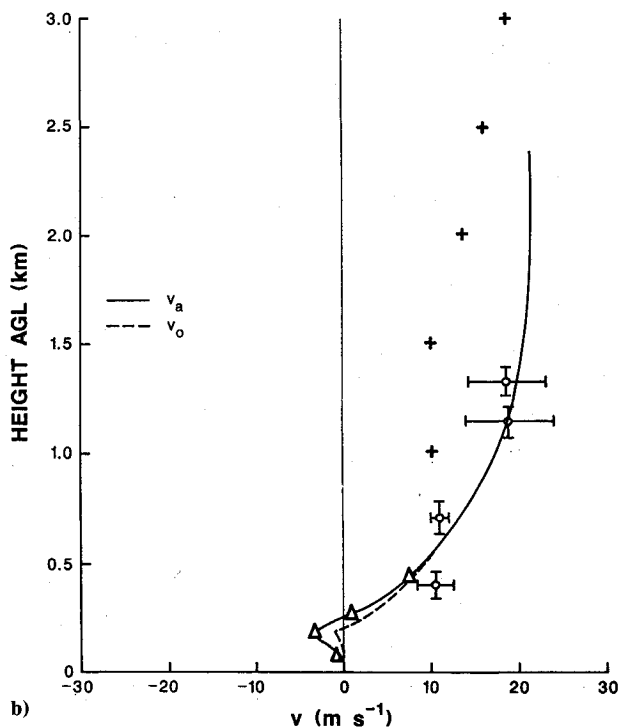
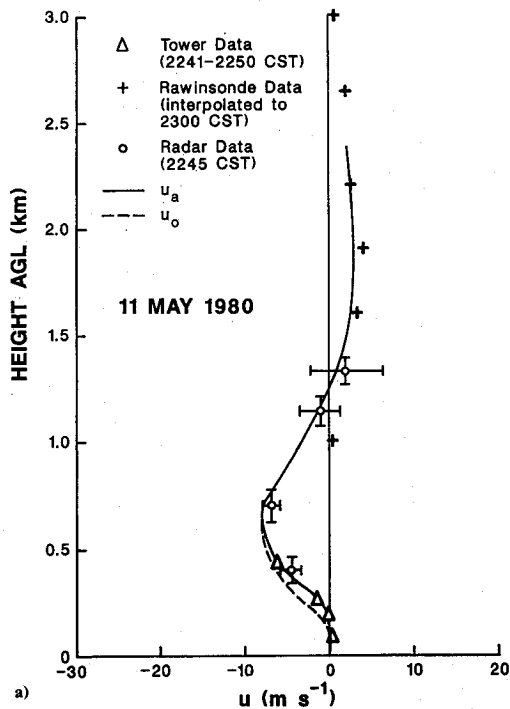


Fig. 4 Ambient wind components perpendicular ( $u$ ) and parallel ( $v$ ) to the front.

$T_s$  the temperature (K) of the parcel when adiabatically cooled to saturation,  $w_s$  the saturation mixing ratio equal to the mixing ratio  $w$  of the parcel since  $w$  is a conserved quantity, and  $c_p$  the specific heat of dry air. The error in  $\theta_e$  computed using this approximate formula can be as large as a few degrees compared to more exact formulas.<sup>28</sup> Although  $\theta_e$  values computed using this approximate formula are not exact, contours of constant  $\theta_e$  can still estimate well the parcel trajectories.

Thus, if the wave is steady and the ambient atmosphere vertically stratified, air parcels travel along surfaces of constant  $\theta_e$ . Contours of equivalent potential temperature (Fig. 5) show a pool of potentially cooler air (shaded area), which suggests that trapped thunderstorm outflow might be recirculating within the wave, whereas the environmental air passes through the wave (or the wave passes through the environ-

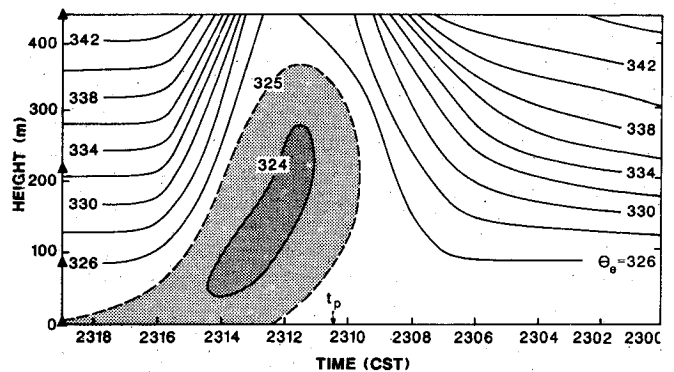


Fig. 5 Equivalent potential temperature in K ( $t_p$  is the time of peak in the  $u$  wind component).

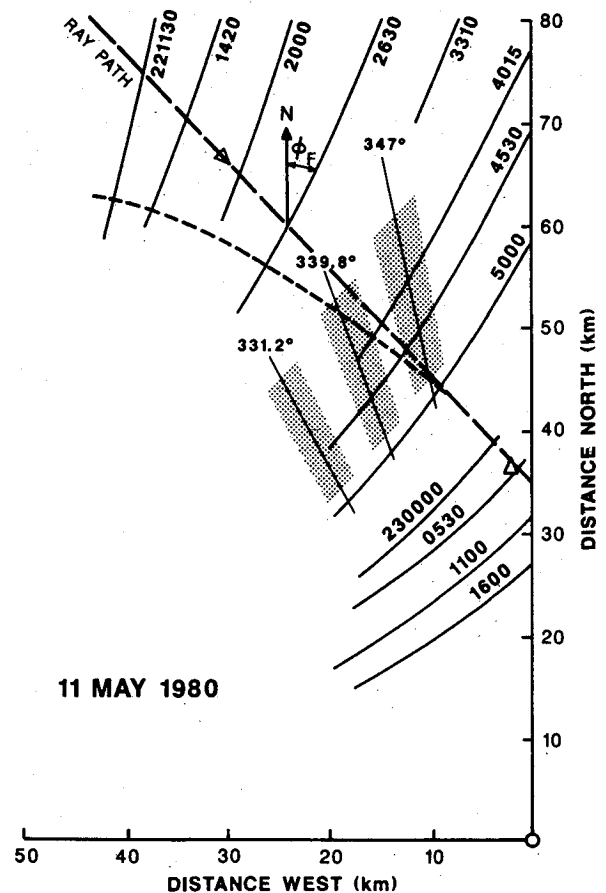


Fig. 6 Isochrones of the leading edge of the solitary wave (KTVY tower location is indicated by  $\Delta$ ; shaded sectors highlight zones from which Doppler data were extracted to determine wave characteristics).

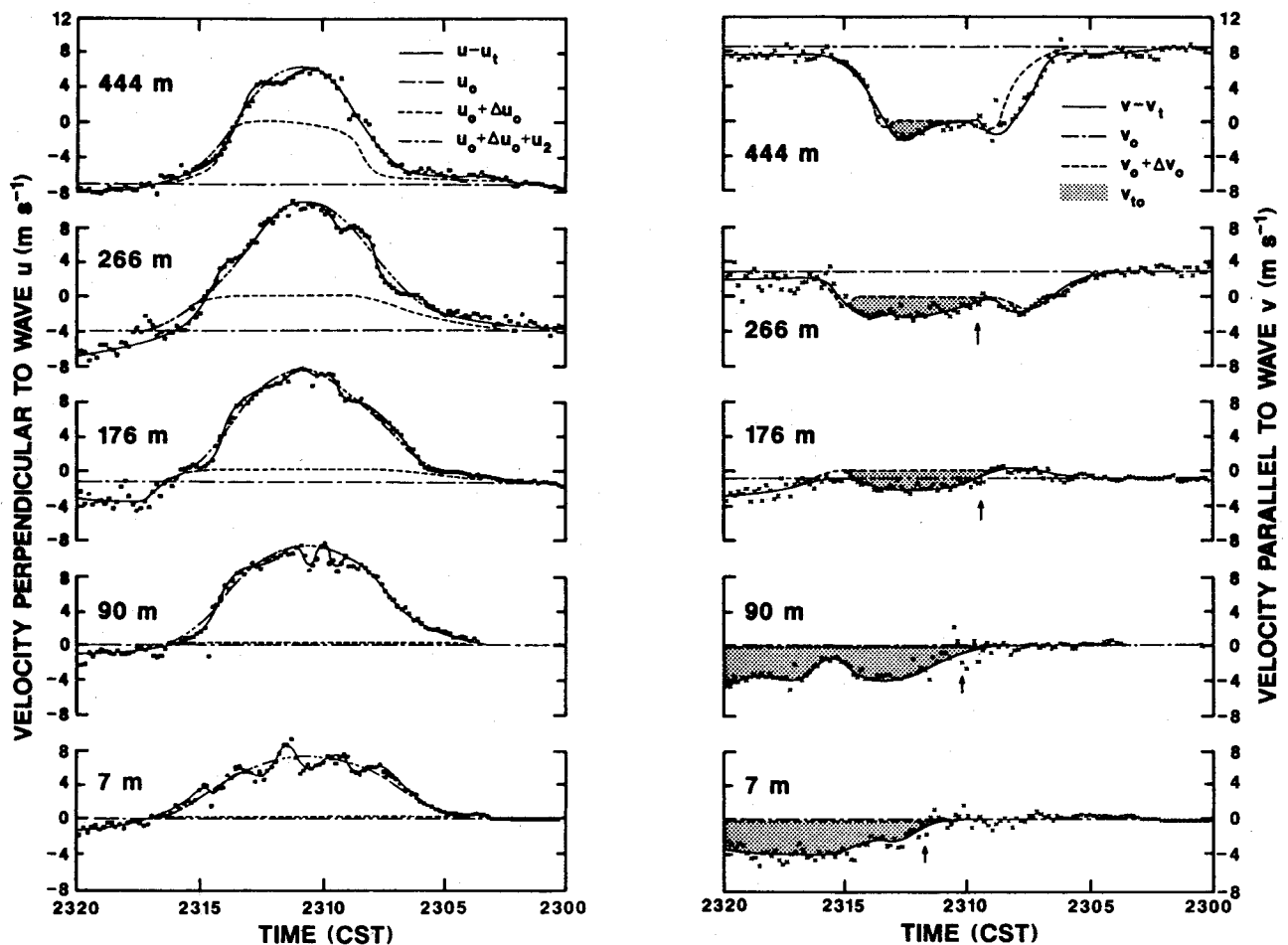


Fig. 7 Samples of wind components at five tower levels, taken at 10 s intervals.

ment) as it is lifted by it. While the  $\theta_p$  contours show a laminar recirculating flow, vertical velocity data from anemometers on the tower suggest the outflow core of the wave is a turbulent blob slowly descending to the ground. Perhaps the trapped air is a cut-off vortex that initially formed at the leading edge of the horizontally spreading density current (i.e., the thunderstorm outflow) when it impacted the stable layer (see the section below on the evolution of thunderstorm-generated solitary waves for further discussion). Once the wave is formed with recirculating outflow inside it, the turbulent outflow eddy is assumed to be trapped by the wave and to continue to propagate at the wave speed, leaving behind an ever-slowing density current. The position of the pool of cool air at the trailing edge of the wave (Fig. 5) is evidence that the heavier outflow is lagging the wave, giving credence to the idea that the wave drags the trapped air or at least that the two have some symbiotic relation. If the trapped air in the wave is formed solely of ambient air and if friction is negligible, the recirculating air should be centered within the wave as the numerical results of Tung et al. indicate.<sup>30</sup>

### Wind Perturbations

Figure 6 shows the position of the leading edge of the Doppler velocity perturbations (i.e., the wave front) caused by the wave as a function of time. This figure indicates that the wavefront passes the KTVY tower at about 23:05 CST. The storm that supposedly created this wave is about 100 km north of the radar at 23:00 CST and is tracking at a supercritical speed to the east-northeast. The short dashed line is the path of the wave front normals through the KTVY tower and the long dashed line is the ray path.<sup>43</sup> A time series of data spaced 10 s apart has been plotted in Fig. 7 to show the temporal

dependence of wind components  $u$  and  $v$  orthogonal to and along the front at five heights. If we ignore the contribution of storm outflow wind (i.e., the shaded areas in Fig. 7), these data exhibit at lower altitudes (i.e.,  $z < 176$  m) a definite short-wavelength solitary perturbation that is nearly wholly in the NW-SE cross section and consequently exhibits the characteristics of a two-dimensional wave. However, at the highest anemometer levels (i.e., 266 and 444 m) pronounced wave-like perturbations appear in both the  $u$  and  $v$  components.

### Components of Wind Change

A close examination of the data suggests that the wind field can be analyzed in terms of six components,

$$v = v_0 + \Delta v_0 + v_2 + v_{t0} + v_{KH} + v_t$$

where  $v_0$  is the background flow assumed to be horizontal in absence of the wave,  $\Delta v_0$  the change caused by the wave when it vertically transports different amounts of  $v_0$  momentum because of  $v_0$  shear,  $v_2$  the wave component associated with perturbations confined to the NW-SE vertical cross section (and, for large amplitude waves, can include recirculating flow as demonstrated by Tung et al.<sup>30</sup>),  $v_{t0}$  the axial (i.e., parallel to the wavefront) component of the trapped thunderstorm outflow,  $v_{KH}$  the velocity of well-defined, short, wavelike perturbations assumed to be Kelvin-Helmholtz (K-H) waves, and  $v_t$  the contribution due to turbulence and other ill-defined, small-scale wind perturbations.

For the sake of argument, we have separated the solitary wave component into two parts:  $v_2$  applicable to regions both within and outside the trapped flow, and a component  $v_{t0}$  assumed perpendicular to  $v_2$  associated only with the trapped

outflow. The orientation of our coordinate frame is selected so that the wave component  $v_2$  lies wholly in the  $x, z$  plane oriented NW-SE. Because the wave generated perturbations in three directions, parcels of air do not follow paths that lie wholly in any vertical plane. Nevertheless,  $v_2$  deduced from estimates of analyzed wind components is equal to  $v_2$  given by theory, which assumes flow solely in the plane perpendicular to the front.

### Wave Guidance of Thunderstorm Outflow: The Leaky Pipe Model

The shaded areas in Fig. 7 are those perturbations that are assumed to be associated with trapped thunderstorm outflow. The arrows there indicate the arrival times of trapped outflow estimated from Fig. 5. It is seen that the onset of wind perturbations associated with trapped outflow (the shaded areas in Fig. 7b) agrees reasonably well with the location of the trapped air inferred from the  $\theta_e = 325$  K contour (Fig. 5) at all tower levels. However, the trapped outflow barely reaches the 444 m level. The spur in the contour of  $\theta_e$ , trailing to the rear of the wave (Fig. 5), is evidence that the pool of cool air is leaking out the rear of the wave in accordance with laboratory observations of fluid flow.<sup>21</sup> The component  $v_{i0}$ , lingering after wave passage, gives evidence that outflow leaking out the rear of the wave is below 90 m.

Although we have deduced that the cool air behind the wave originates in the wave, one might conjecture that it is a density current and what appears to be a solitary wave is really a current head of remarkably large amplitude. The ratio of density current head heights to the depth of the current behind the head, recently measured with radar for 25 cases, shows an average value of 1.14 and a maximum observed ratio of 1.35.<sup>31</sup> Drogemeier and Wilhelmson, working with numerical models of density currents, showed ratios as large as about two.<sup>32</sup> If the wave reported herein is the head of an advancing current, its height is about 400 m and the depth of the current behind it is less than 100 m; it has a ratio larger than 4, an unusual value. Although this observation alone cannot preclude this shallow layer of cool air from being a density current, more evidence against this hypothesis is provided by the observation that the relative winds in this layer are away from the front at all levels. Further support is derived from the disparity between the observed speed of the wavefront and that theoretically deduced for density current fronts. That is, because the depth of the current is less than 100 m and the difference in virtual potential temperature is, at most,  $0.8^\circ\text{C}$ , the speed  $c_g = \sqrt{gh\Delta\theta_v/\theta_v(0)}$  of the current's front computes to be less than 2 m/s. This is markedly less than the observed speeds that are larger than 12 m/s.

### Wind Perturbations Produced by Vertical Transport of Horizontal Momentum

The  $\Delta u_0$  and  $\Delta v_0$  components in Fig. 7 are estimated by assuming that parcels of air, traveling along lines of constant  $\theta_e$  (Fig. 5), do not change their horizontal momentum. Contours of  $\theta_e$  should give an accurate depiction of parcel trajectories if the flow is steady and if the atmosphere is horizontally homogeneous. For example, Fig. 5 suggests that air from a height of about 100 m above ground is lifted by the wave to the 444 m altitude of the topmost anemometer. The pair of negative peaks seen in the  $(v_0 + \Delta v_0)$  trace (Fig. 7b, top) is most likely generated as air, having the peak negative  $v_0$  from the 176 m level (see Fig. 4b), passes twice through the anemometer at the 444 m level. Moreover, the computed shape and amplitude of the waveform  $(v_0 + \Delta v_0)$ , at the 444 m level, where the only contributions to changes in  $(v - v_i)$  are from the vertical transport of momentum, agree remarkably well with the observed shape and amplitude. The good agreement of the observed data  $v$  and the wind change deduced from Figs. 4 and 5 suggest that turbulence is weak (i.e., rms values are less than about 0.5 m/s) and that  $v_{KH} = 0$  at the 444 m level. However,

at the 90 m level, K-H waves might be the cause of the wave-like perturbation in the  $v$  component of wind. Kelvin-Helmholtz billows are frequently observed along the trailing edge of solitary wave roll clouds seen over the southern margin of the Gulf of Carpentaria in northern Australia.<sup>19</sup>

To compare observations with two-dimensional theory, we assume that  $u - u_i - u_{KH}$  (dashed/double-dotted lines in Fig. 7a) is equal to the sum of  $\Delta u_0$  due to wave-induced vertical transport of the  $u_0$  momentum, ambient flow  $u_0$ , and wave component  $u_2$  obtained from two-dimensional theory. The dashed/double-dotted curves are subjectively estimated to filter turbulence and the apparent wave disturbances that appear to develop in the solitary wave.

Near the ground, there is no lifting of air so  $\Delta u_0 = 0$ . Hence, the wave component  $u_2$  is well estimated from the dashed/double-dotted curve. Moreover, vertical velocity data show weak lifting below 90 m (as does Fig. 5) and, because the vertical shear of  $u_0$  is nearly zero below 100 m (Fig. 4a),  $u_2$  is also given by the dashed/double-dotted curve at the 90 m tower level. However, at the 266 m level,  $u_0$  is about  $-4$  m/s and air of zero momentum is lifted from near the 100 m level, so we can expect that  $\Delta u_0$  has a peak of about 4 m/s. The dashed lines on Fig. 7 are the estimates of  $(u_0 + \Delta u_0)$  obtained from Figs. 4a and 5. At the 444 m level,  $u_0$  is much more negative (i.e.,  $-7$  m/s) and, because air from near the 100 m level is also brought to this topmost tower level, the peak change in  $\Delta u_0$  should be about 7 m/s, as is sketched in Fig. 7a.

### Comparison of Observed Waveforms with Theory

To compare observed waveform with theory,  $u_2(t)$  data obtained from Fig. 7 for each minute of observation at the 266 and 444 m heights on the tower are plotted in Fig. 8. Also plotted in this figure are the theoretical waveforms (solid lines) given by weakly nonlinear theory.<sup>33</sup> Although evidence of trapped outflow suggests the wave might be strongly nonlinear, it is interesting that the observed waveforms agree well with the analytical expression (solid line) deduced from nonlinear theory. Chen compared vertical wave velocities with those determined by theory and found very good agreement.<sup>34</sup> However, we notice that the wind data at 444 m above ground level suggest a faster decrease of  $u_2$  at the extremities of the wave. At the height of 266 m (and also at lower heights),  $u_2(t)$  data show the wave crest to be more rounded and the sides to be steeper than indicated by theory. This could be anticipated because the numerical results of Tung et al.<sup>30</sup> show that strongly nonlinear waves do have more rounded crests and steeper sides. Furthermore, Cummins and Le Blond<sup>35</sup> compared waveforms of observed oceanic solitary waves with those shapes produced by weakly nonlinear theories and they also found, in all cases, that the observed waveforms exhibited more rounded crests and steeper sides. As in the case of the

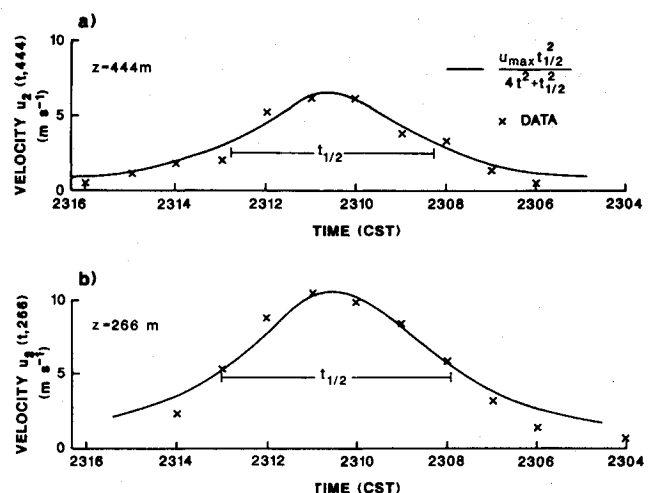


Fig. 8 Comparison of weakly nonlinear theory and observed waveform.

atmospheric solitary wave examined herein, the oceanic waves had amplitudes that violated weakly nonlinear assumptions. Therefore, the departure of the observed waveform from that given by weakly nonlinear theory might be explained by the large amplitude of the observed wave.

### Scenario for Evolution of Thunderstorm-Generated Solitary Waves

Data suggest that the observed solitary wave had trapped thunderstorm air that was cooler and drier than the wave's ambient environment and thus, being more dense, leaked out the rear of the wave. The presence of this cool pool of air left behind the wave can complicate the interpretation of measurements if they are made only with instruments near the ground, because temperature drop and wind shift data might be misinterpreted as evidence of an advancing density current. However, observations with the tall tower and Doppler radar show that this pool of very shallow air (less than 100 m) leaked out of the wave. Furthermore, the parent storm provides unexpected support for the solitary wave as outflow is guided by the wave and flows continuously along the wave's axis away from the storm.

It is remarkable that the storm outflow remained in the wave for distances of at least 60 km from the storm. Although storm outflows propagate as density currents to large distances, it is suggested that gravity waves (and, in particular, solitary waves formed by the interaction of the storm's downdraft with the stable layer) can transport the outflow faster and probably, with greater momentum, farther. Thus, hazardous shear, normally confined to regions beneath downdrafts, might indeed be found at large distances from them.

The results of this study and the observations of Linden and Simpson<sup>13</sup> suggest a scenario for the evolution of the solitary wave (Fig. 9). A thunderstorm downdraft generates a density current and a horizontal rotor at its leading edge. If the current and its rotor are also imbedded in an inversion layer, they launch one or more wave-like disturbances that grow and propagate at speeds determined by the wave amplitude and vertical profile of the wind and the virtual potential temperature of the ambient environment. The density current front has a speed that is dependent on the depth of the current and, because this depth is continually decreasing, the wave eventually propagates ahead, leaving the residual current behind. As the wave propagates away from the current, it drags along a horizontal vortex of thunderstorm outflow, separating it from its source. The wave and circulating outflow air continue to propagate away at velocities faster than the current's front, thus leaving it farther and farther behind. The recirculating trapped air in the wave creates strong shear near the Earth's surface. However, as the trapped outflow slowly leaks out the rear of the wave, leaving behind a shallow pool of cool air, the wave amplitude decreases. After the outflow air is completely

gone, the wave can continue on as a wave of permanent form, if the energy loss due to ground friction and radiation can be ignored. If the part of the troposphere overlying the inversion layer is not neutrally stable, wave energy will be radiated away from the inversion layer.<sup>23</sup>

### Wind Shear Hazard Potential

Although the observed solitary wave reported herein was 60 km (32 n. mi.) from the storm that apparently generated it, it still contained significant horizontal and vertical shears (e.g.,  $4.4 \times 10^{-3}$  and  $60 \times 10^{-3}$  s) of the horizontal wind 90 m (300 ft) above the ground. The horizontal shear persisted over a distance of about 1500 m (i.e.,  $\approx \frac{3}{4}$  n. mi.). Short-wavelength waves, which developed atop this solitary wave, intensified the horizontal shear to  $7.6 \times 10^{-3}$  s over a distance of 700 m (0.4 n. mi.). For a perspective on the significance of such shears on aircraft performance, note that a decrease in head wind along a southeastward 3 deg glide slope into the solitary wave is larger (38 knots or 19 m/s) than the one (35 knots or 17.5 m/s) that caused a 50 m (150 ft) drop in altitude of a Boeing 747 aircraft on its approach into Melbourne, Australia.<sup>36</sup> Turbulence behind the wave possessed even stronger horizontal shears with wind changes as large as 6 m/s (12 knots) over a 130 m (400 ft) distance or a shear value near  $50 \times 10^{-3}$  s. An aircraft landing at a speed of 72 m/s (140 knots) could experience a 6.2 m/s (12 knots) head wind decrease in  $\sim 2$  s. These large solitary wave shears were observed at the tall tower site when the storm was 60 km away. At points closer to the storm, the shear should be significantly larger. For example, the wave amplitude observed by Doppler radar at 22:45 CST for locations 45 km from the storm's edge was almost double that observed at the tower.<sup>37</sup> It should be emphasized that thunderstorm-generated waves of much larger amplitude than that described here and with proportionally more intense shear have been observed.<sup>9</sup>

The only documented flights of an aircraft through large-amplitude solitary waves occurred on Sept. 29 and Oct. 4, 1979.<sup>38</sup> The aircraft, a Beechcraft Travelair, was directed to make measurements in morning glories over the Gulf of Carpentaria off the northern coast of Australia. The pilot was instructed to fly at constant altitude and power through these glories and often found himself on first an upward and then a downward current causing the aircraft to ascend and descend

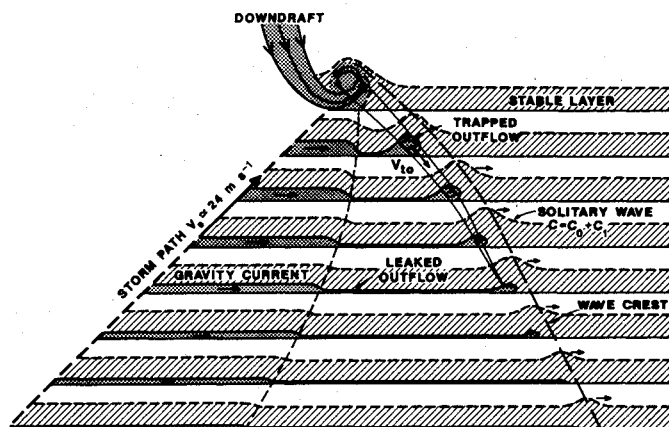


Fig. 9 Scenario for the evolution of the thunderstorm-generated solitary wave.

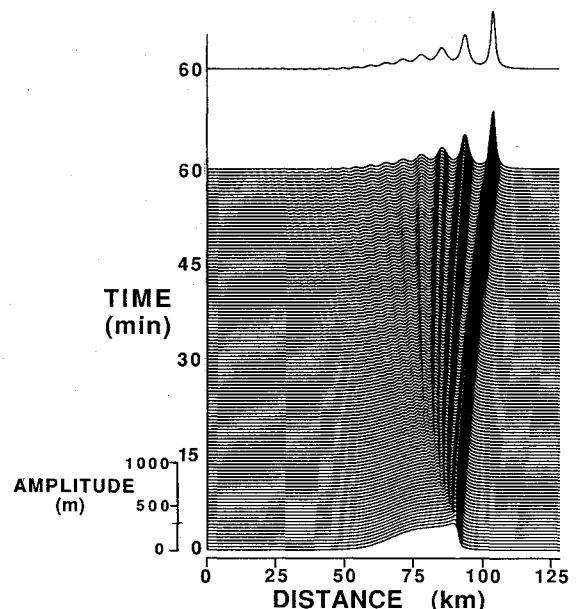


Fig. 10 Wave-induced vertical displacement of air vs position along the direction of propagation with time as a parameter. The coordinate system moves at the speed  $C_0$  (11.1 m/s or 22.2 knots), the fastest that waves of infinitesimal amplitude can propagate.



at rates as high as 600 m/min (2000 ft/min). During the traverse of the leading solitary wave on Oct. 4, the pilot was forced to pull out when he was within 50 m (150 ft) of the sea. This wave originated in the collision of opposing sea breeze fronts over the Cape York peninsula<sup>39,40</sup> and not in thunderstorm activity. Yet it produced significant shear that was hazardous to safe flight, even though it was more than 300 km from its source. It should be noted, however, that the wave on Oct. 4 is not a particularly large-amplitude disturbance. For example, the surface pressure perturbation corresponding to the leading disturbance amounted to only about 0.8 mbar. Morning glory solitary waves of much larger amplitude (>2.5 mbar) have been observed. In this regard, the flight through the disturbance on Sept. 29 is of interest in that it was a somewhat larger disturbance (1.4 mbar) with significantly more intense shear. The minimum altitude traverse through this disturbance was, however, carried out at a height of 600 m. Even so, the aircraft suffered a drop in altitude of more than 200 m, which is hardly trivial. A later attempt (1982) to fly through one of these phenomena was frustrated by the pilot who refused to fly into the wave after he had seen it (R.H. Clarke, private communication).

Christie and Muirhead<sup>18</sup> showed how an initially long wave with relatively benign shear can evolve under the influence of nonlinearities and frequency dispersion into an amplitude-ordered family of solitary waves of large-amplitude and shorter half-amplitude widths, in which the shear hazard is markedly increased. Their work suggests that the intense, transient shear zones generated with these waves constitute a serious hazard to the safety of flight at low altitudes.

A recent theoretical study<sup>22</sup> of nonlinear dispersive wave disturbances has shown that, under ideal atmospheric waveguide conditions and when the initial disturbance has large volume, the ratio of the amplitude of the leading solitary wave to the amplitude of the initial disturbance approaches a limiting value of 4.0. This investigation has also shown that the formation of solitary waves is a surprisingly rapid process; well-developed solitary waves with their characteristic intense wind shear patterns can be created over a distance of some tens of kilometers. As an illustration, Fig. 10 shows the results of a numerical integration of the Benjamin-Davis-Ono equation, the governing equation for the evolution of long nonlinear waves in the atmosphere, for a relatively small-amplitude and longer-wave initial disturbance propagating as a bore in a simple, but realistic, boundary-layer waveguide in which the Brunt-Väisälä frequency is determined by  $N^2(z) = N_0^2 \operatorname{sech}^2(z/H)$ , with  $N_0 = 0.0314 \text{ s}^{-1}$  and an effective depth  $H$  of 500 m (1500 ft). Well-developed waves of short wavelength are evident after about 20 min, by which time the leading edge of the disturbance has progressed some 14 km (9 mi) from its initial position. The offset trace in Fig. 10 illustrates the nearly asymptotic form attained by the leading solitary wave at the 1 h mark when its speed is nearly 16 m/s (32 knots) and its has propagated a total distance close to 55 km (34 mi). It is worth noting that the evolution of short solitary wave components from a longer-wave disturbance occurs more rapidly when the initial wave has larger amplitude. Cylindrical solitary waves, forced by a divergent outflow, might grow faster yet because of vortex stretching.<sup>13</sup> Thus, a relatively benign initial wind shear event, one having a step-like change in wind that should cause aircraft only to overshoot the runway irrespective of its approach into the disturbance, can change quickly to one whereby wind shear is significantly bimodal and more dangerous, depending upon the pilot's reaction to wind changes. Although Fig. 10 shows the wave to grow to an asymptotic form, losses due to radiation, leakage, and turbulence should cause the wave to reach a peak amplitude, whereafter the wave intensity will diminish.

To determine whether thunderstorm generated gravity waves have caused any U.S. aircraft accidents in the past, we now review the paper of Rudich,<sup>41</sup> who summarized the weather conditions leading to 33 weather-involved air carrier

accidents that have been investigated and formally reported on by the National Transportation Safety Board for incidents that occurred during the period 1962–1984. In 11 of the 18 fatal crashes, wind shear was implicated, but altogether there were 26 accidents causing injuries and/or damage to the aircraft in which wind shear may have been the cause or the contributing cause of the accident. In nine of the fatal cases (seven of the nonfatal ones), the aircraft either penetrated thunderstorm rain or was in the area of thunderstorm rain. In one case, the aircraft flew through heavy rain, but thunder was not reported. If thunderstorm-generated, large-amplitude gravity waves were involved in these accidents, they would likely be in their earliest stage of formation; but, of course, it is at the time when these waves might have the largest amplitude. For example, a large amplitude, wave-like perturbation or rotor is deduced to be in the outflow of the thunderstorm that caused the crash of Delta flight 191 at the Dallas/Fort Worth International Airport on Aug. 2, 1985.<sup>42</sup> In only one fatal accident was wind shear noted as a possible cause without rain being mentioned, so waves might have been present. In two of the fatal cases, it was reported that the aircraft was near, or had entered, a roll cloud that was in advance of a squall line producing moderate rain. The presence of a roll cloud is strong evidence for the existence of a horizontal rotor and the formation of a solitary wave. In eight of the nonfatal accidents, there were no reported thunderstorms in the vicinity of the accident, and thus gravity waves or wave-induced turbulence might have been the cause or contributing cause of the accidents. Therefore, ignoring the cases involving thunderstorm rain in which microbursts are likely to be the cause, gravity waves might be implicated in at least 11 of the 33 investigated accidents.

## Conclusions

Although we have no conclusive evidence to date that solitary or gravity waves have been a cause or a contributing cause of fatal accidents, the data, as meager as they are, suggest that horizontal rotors at the leading edge of thunderstorm gravity currents (often called gust fronts) and strongly nonlinear waves can pose a hazard to safe flight and may have caused accidents. Large-amplitude, short-wavelength solitary waves can propagate far distances with little loss in amplitude and might also pose a wind shear hazard in areas far removed from thunderstorm activity. Thus, internal gravity waves should be studied both experimentally and theoretically. Furthermore, because it is the strongly nonlinear waves that pose the threat, theoretical studies should resort to numerical models. Experiments must employ equipment, such as tall towers, Doppler radar, and aircraft, that can provide the unambiguous observations far above the ground.

## Acknowledgments

Many thanks to Susumu Kato, Director of the Radio Atmospheric Science Center, Kyoto University, Japan, for inviting R. J. Doviak to lecture on Doppler radar and weather observations, because it was during the January–March 1987 period that much of the research reported here was accomplished. Messrs. Michael Eilts and Kevin Thomas contributed to the presentation of tower data and Mr. Steve Smith provided the radar-derived wind profiles. Dr. Dusan S. Zrnic' has been most helpful in his review and encouragement and initiated the idea of thunderstorm outflow propagating in the "guidance pipe" formed by the solitary wave. Thanks to Dr. R. H. Clarke, (ret.) Chief of the Division of Atmospheric Physics, CSIRO, Melbourne, Australia, for sharing with us his unpublished observations. Ms. Joan Kimpel provided graphic services and Ms. Carole Holder prepared the typescript. The Federal Aviation Administration supported this work under Contract DTFA01-80-Y-10524. One of the authors (D. R. Christie) was supported in part by the U.S. Air Force Office of Scientific Research under Contract AFOSR-83-0045.



## References

- <sup>1</sup>Doviak, R. J. and Zrnic, D. S., *Doppler Radar and Weather Observations*, Academic Press, Orlando, FL, 1984.
- <sup>2</sup>McCaul, E. W., Bluestein, H. B., and Doviak, R. J., "Airborne Doppler Lidar Observations of Convective Phenomena in Oklahoma," *Journal of Atmospheric and Oceanic Technology*, Vol. 4, No. 3, 1987, pp. 479-497.
- <sup>3</sup>Carter, J. K., "The Meteorological Instrumented WKY-TV Tower Facility," Oper. Div., National Technical Information Service, Springfield, VA, NSSL Tech. Memo. 50, 1970 (NTIS COM-71-00100).
- <sup>4</sup>Kessler, E., "Wind Shear and Aviation Safety," *Nature*, Vol. 315, No. 6016, 1985, pp. 179-180.
- <sup>5</sup>Fujita, T. T., "The Downburst," Dept. of Geophysical Science, University of Chicago, Chicago, SMRP Rept. 210, 1985.
- <sup>6</sup>McCarthy, J., Wilson, J. W., and Fujita, T. T., "The Joint Airport Weather Studies Project," *Bulletin of the American Meteorological Society*, Vol. 63, 1982, p. 15-22.
- <sup>7</sup>Byers, H. R. and Braham, R. R., Jr., "The Thunderstorm," Report of the Thunderstorm Project, U.S. Government Printing Office, Washington, DC, 1949.
- <sup>8</sup>Lee, J. T., Stokes, J., Sasaki, Y., and Baxter, T., "Thunderstorm Gust Fronts—Observations and Modeling," Systems Research and Development Service, Federal Aviation Administration, Washington, DC, 1978.
- <sup>9</sup>Fulton, R., "Observations of the Interactions of a Nocturnal Thunderstorm Outflow with a Stable Environment," M.S. Thesis in Meteorology, University of Oklahoma, Norman, 1987.
- <sup>10</sup>Doviak, R. J., and Ge, R. S., "An Atmospheric Solitary Gust Observed with a Doppler Radar, a Tall Tower and a Surface Network," *Journal of the Atmospheric Sciences*, Vol. 41, 1984, pp. 2559-2573.
- <sup>11</sup>Goff, R. C., "Low Level Wind Shear Alert System (LLWAS)," National Aviation Facilities Experimental Center, Atlantic City, NJ, Rept. FAA-RD-80-45, 1980.
- <sup>12</sup>von Kármán, T., "The Engineer Grapples with Nonlinear Problems," *Bulletin of the American Mathematical Society*, Vol. 46, 1940, pp. 615-683.
- <sup>13</sup>Linden, P. F., and Simpson, J. E., "Microbursts: A Hazard for Aircraft," *Nature*, Vol. 317, Oct. 1985, pp. 601-602.
- <sup>14</sup>Stewart, O., *Danger in the Air*, Philosophical Library, New York, 1958, pp. 53-63.
- <sup>15</sup>Christie, D. R. and Muirhead, K. J., "Solitary Waves: A Hazard to Aircraft Operating at Low Altitudes," Research School of Earth Sciences, Australian National University, Rept., 1982.
- <sup>16</sup>Gossard, E. E., "Aircraft Hazard Assessment from a Clear-Air Radar and Meteorological Tower Study of Gravity Wave Events," U.S. National Oceanic and Atmospheric Admin., Boulder, CO (Doc. PB83-257139, National Technical Information Service, Springfield, VA 22161), 1983.
- <sup>17</sup>Christie, D. R., Muirhead, K. J., and Clarke, R. H., "Solitary Waves in the Lower Atmosphere," *Nature*, Vol. 293, No. 5827, 1981, pp. 46-49.
- <sup>18</sup>Christie, D. R. and Muirhead, K. J., "Solitary Waves: A Hazard to Aircraft Operating at Low Altitudes," *Australian Meteorological Magazine*, Vol. 31, 1983, pp. 97-109.
- <sup>19</sup>Christie, D. R. and Muirhead, K. J., "Solitary Waves, a Low-Level Wind Shear Hazard to Aviation," *International Journal of Aviation Safety*, Vol. 1, Sept. 1983, pp. 169-190.
- <sup>20</sup>Christie, D. R. and Muirhead, K. J., "Solitary Waves and Low-Altitude Wind Shear in Australia," *Aviation Safety Digest*, No. 123, 1985, pp. 3-8.
- <sup>21</sup>Maxworthy, T., "On the Formation of Nonlinear Internal Waves from Gravitational Collapse of Mixed Regions in Two and Three Dimensions," *Journal of Fluid Mechanics*, Vol. 96, 1980, pp. 47-64.
- <sup>22</sup>Christie, D. R., "Long Nonlinear Waves in the Lower Atmosphere," *Journal of the Atmospheric Sciences*, to be published March or April 1989.
- <sup>23</sup>Crook, N. A., "The Effect of Ambient Stratification and Moisture on the Motion of Atmospheric Undular Bores," *Journal of the Atmospheric Sciences*, Vol. 43, No. 2, 1986, pp. 171-181.
- <sup>24</sup>Farnsworth, T. H., "Discussing Wind Shear, Causes and Effect of Rough Air Phenomenon," *Skyways*, Henry Publications, New York, 1960, pp. 42-43.
- <sup>25</sup>Fujita, T. T., "DFW Microburst," Dept. of Geophysical Science, University of Chicago, Chicago, SMRP Research Paper 217, 1986.
- <sup>26</sup>Anderson, K. W. and Clark, B. A. J., "Wind Shear in Australia," *Aviation Safety Digest*, Vol. 106, 1979, pp. 14-20.
- <sup>27</sup>Anderson, K. W. and Clark, B. A. J., "A Study of Wind Shear Effects on Aircraft Operations and Safety in Australia," Aeronautical Research Lab., Dept. of Defense, Melbourne, Victoria, Aust., Systems Rept. 24, 1981.
- <sup>28</sup>Bolton, D., "The Computation of Equivalent Potential Temperature," *Monthly Weather Review*, Vol. 108, 1980, pp. 1046-1053.
- <sup>29</sup>Holton, J. R., *An Introduction to Dynamic Meteorology*, Academic Press, New York, 1972.
- <sup>30</sup>Tung, K. K., Chan, T. F., and Kubota, T., "Large Amplitude Internal Waves of Permanent Form," *Studies in Applied Mathematics*, Vol. 66, 1982, pp. 1-44.
- <sup>31</sup>Mahoney, W. P. III, "Gust Front Characteristics and the Kinematics Associated with Interacting Thunderstorm Outflows," *Monthly Weather Review*, Vol. 116, No. 5, 1988.
- <sup>32</sup>Droegemeier, K. K. and Wilhelmson, R. B., "Numerical Simulation of Thunderstorm Outflow Dynamics," *Journal of the Atmospheric Sciences*, Vol. 44, No. 8, 1987, pp. 1180-1210.
- <sup>33</sup>Benjamin, T. B., "Internal Waves of Permanent Form in Fluids of Great Depth," *Journal of Fluid Mechanics*, Vol. 29, 1967, pp. 559-592.
- <sup>34</sup>Chen, S., "A Theoretical Analysis and Comparison of the Theory and Observation of Wind and Pressure Fields in an Atmospheric Solitary Wave," M.S. Thesis, Dept. of Meteorology, University of Oklahoma, Norman, 1985.
- <sup>35</sup>Cummins, P. F. and Le Blond, P. H., "Analysis of Internal Solitary Waves Observed in Davis Strait," *Atmosphere—Ocean*, Vol. 22, No. 2, 1984, pp. 173-192 (Canadian Meteorological and Oceanic Society).
- <sup>36</sup>Woodfield, A. A., "Wind Shear and Vortex Wake Research in U.K. 1982," *Proceedings of Sixth Annual Workshop on Meteorological and Environmental Inputs to Aviation Systems*, edited by W. Frost and D. W. Camp, NASA Rept. CP-2274 and U.S. Dept. of Transportation Rept. DOT/FAA/RD-82/72, 1983, pp. 66-83.
- <sup>37</sup>Doviak, R. J. and Chen, S., "Observations of a Thunderstorm Generated Gust Compared with Solitary Wave Theory," Systems Res. and Dev. Service, Federal Aviation Administration, Washington, DC, FAA Rept. DOT F1700.7, 1988.
- <sup>38</sup>Clarke, R. H., Smith, R. K., and Reid, D. G., "The Morning Glory of the Gulf of Carpentaria: An Atmospheric Undular Bore," *Monthly Weather Review*, Vol. 109, 1981, pp. 1726-1750.
- <sup>39</sup>Noonan, J. A. and Smith, R. K., "The Generation of North Australian Cloud Lines and the 'Morning Glory'," *Australian Meteorological Magazine*, Vol. 35, 1987, pp. 31-45.
- <sup>40</sup>Clarke, R. H., "Colliding Sea-Breezes and the Creation of Internal Atmospheric Bore Waves: Two-Dimensional Numerical Studies," *Australian Meteorological Magazine*, Vol. 1984, pp. 207-226.
- <sup>41</sup>Rudich, R. D., "Weather-Involved U.S. Air Carriers Accidents 1962-84—A Compendium and Brief Summary," AIAA Paper 86-0327, Jan. 1986.
- <sup>42</sup>Caracena, F., "The Crash of Delta Flight 191 at Dallas-Fort Worth International Airport on 2 August 1985: Multiscale Analyses of Weather Conditions," National Oceanic and Atmospheric Administration, Tech. Rept. ERL 430-ESG 2, 1986.
- <sup>43</sup>Doviak, R. J. and Thomas, K. W., "The Wave Front Shape and Position of a Great Solitary Wave of Translation," *Proceedings of International Geo-Science and Remote Sensing Symposium*, Sept. 1988.